

## Supporting information

### **OFF-ON nanodiamond drug platform for targeted cancer imaging and therapy**

Shiguo Wei,<sup>a</sup> Lin Li,<sup>b</sup> Xiangbin Du,<sup>a</sup> and Yingqi Li<sup>a,b\*</sup>

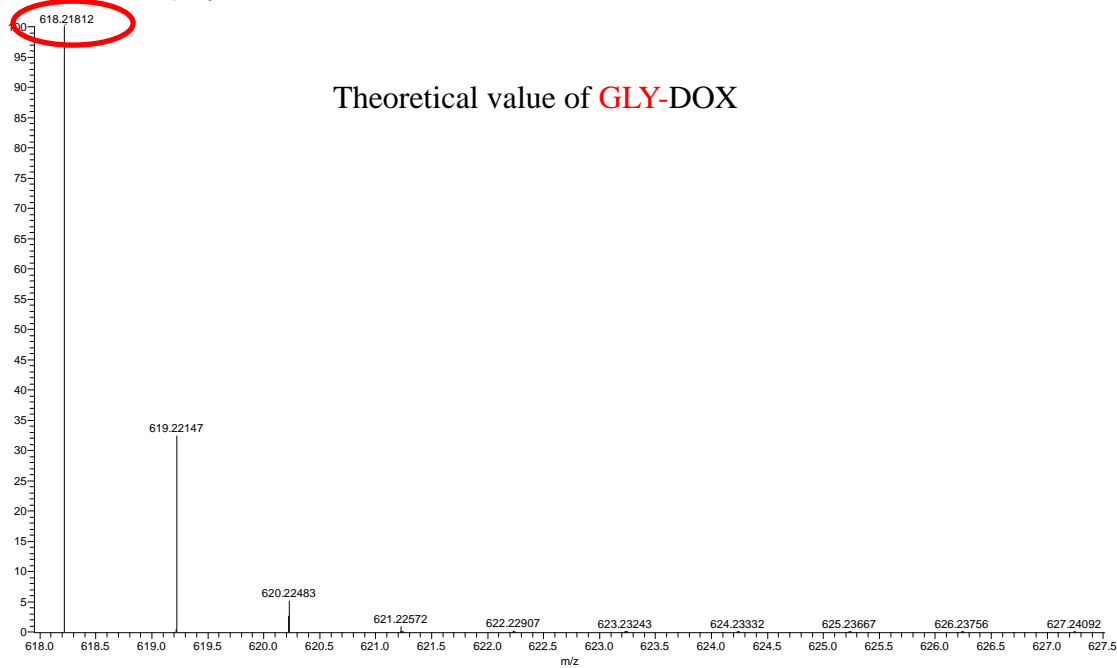
<sup>a</sup> Department of Chemistry, School of Chemistry and Chemical Engineering, Shanxi University, Taiyuan 030006, PR China.

<sup>b</sup> Key Laboratory of Chemical Biology and Molecular Engineering of Ministry of Education, Institute of Molecular Science, Shanxi University, Taiyuan 030006, PR China.

#### **Corresponding author**

\* E-mail: wkyqli@sxu.edu.cn; Tel.: +86 351 7010588

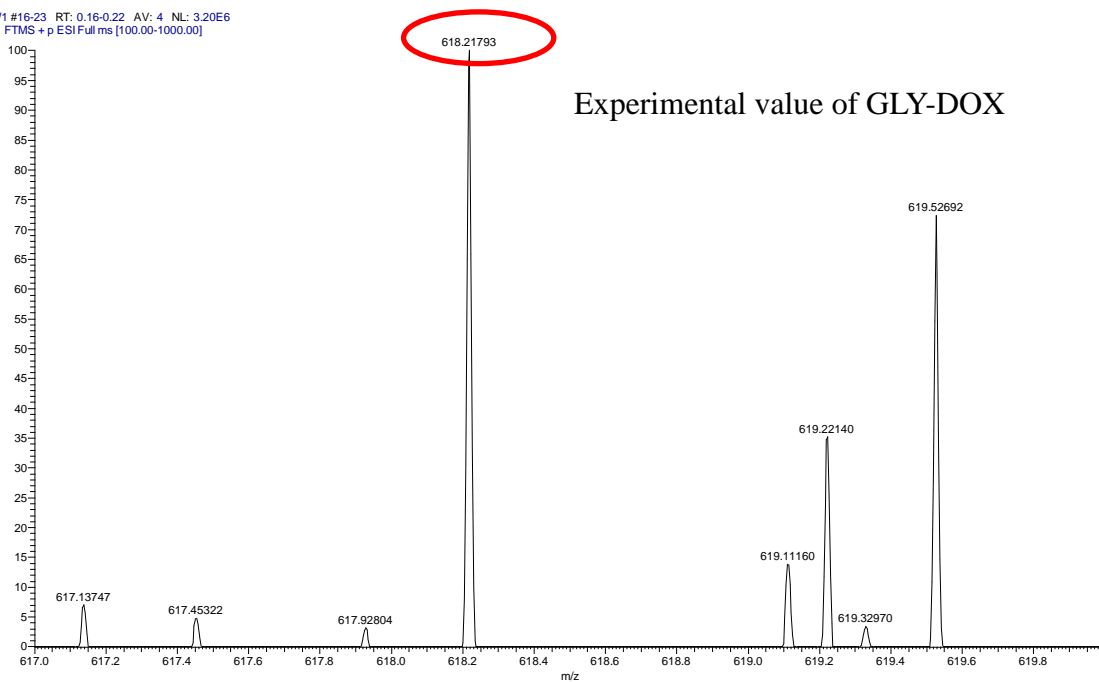
C30H35NO13 +H, C30 H36 N1 O13 pa Chrg 1



HRMS of free GLY-DOX

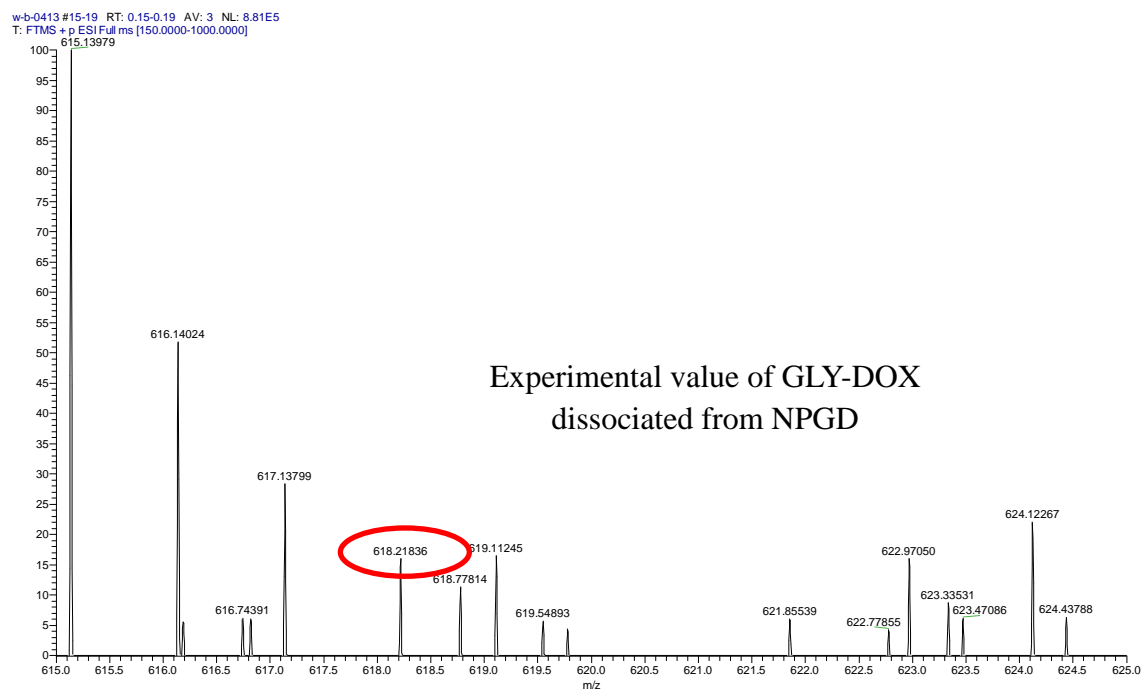
A

W1 #16-23 RT: 0.16-0.22 AV: 4 NL: 3.20E6  
T: FTMS + p ESI Full ms [100.00-1000.00]



HRMS of prepared DOX-GLY

**B**



HRMS of GLY-DOX dissociated from NPGD in ABS (pH 4.5)

**Fig. S1** HRMS of prepared GLY-DOX or GLY-DOX dissociated from NPGD in ABS (pH 4.5). (A) HRMS (ESI, m/z):  $[M + H]^+$  Calcd for  $C_{30}H_{36}NO_{13}$ : 618.21812, found 618.21793. (B) HRMS (ESI, m/z):  $[M + H]^+$  Calcd for  $C_{30}H_{36}NO_{13}$ : 618.21812, found 618.21836.

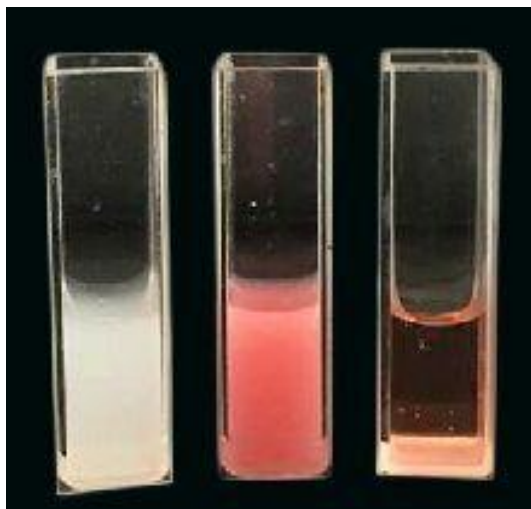


**Fig. S2** The photographs in the PBS (pH 7.4) buffer solution of ND-PEG, NPGD and free DOX in left-to-right order.

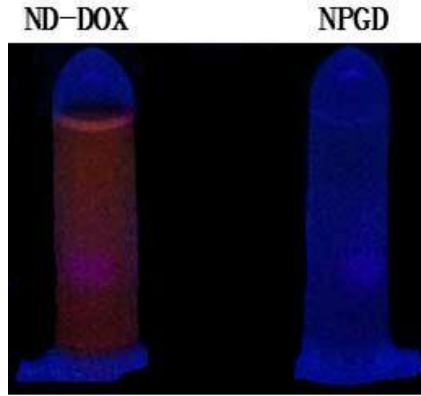


**Fig. S3** The photographs in the PBS solutions of ND-DOX (physical adsorption) and NPGD (ester linkage) in UV light.

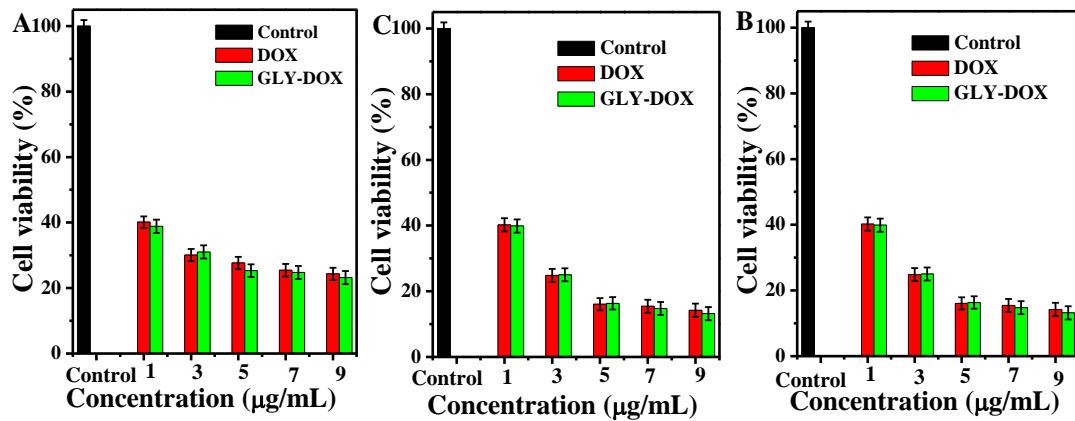


**Fig. S4** Effect of GLY-DOX and DOX on HepG2, HeLa and MCF-7 cells viability for 72 h were measured by MTT assay. (A) HepG2 cells, (B) HeLa cells and (C) MCF-7 cells. Experiments were repeated three times and data are presented as the mean  $\pm$  SD (for each group, n = 6).

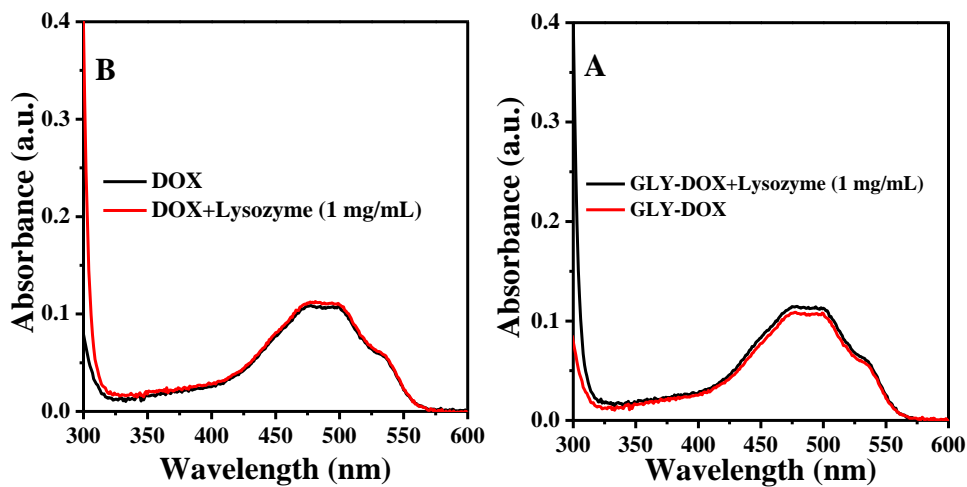


**Fig. S5** The effect of lysozyme on the GLY-DOX and DOX by UV-vis spectra.

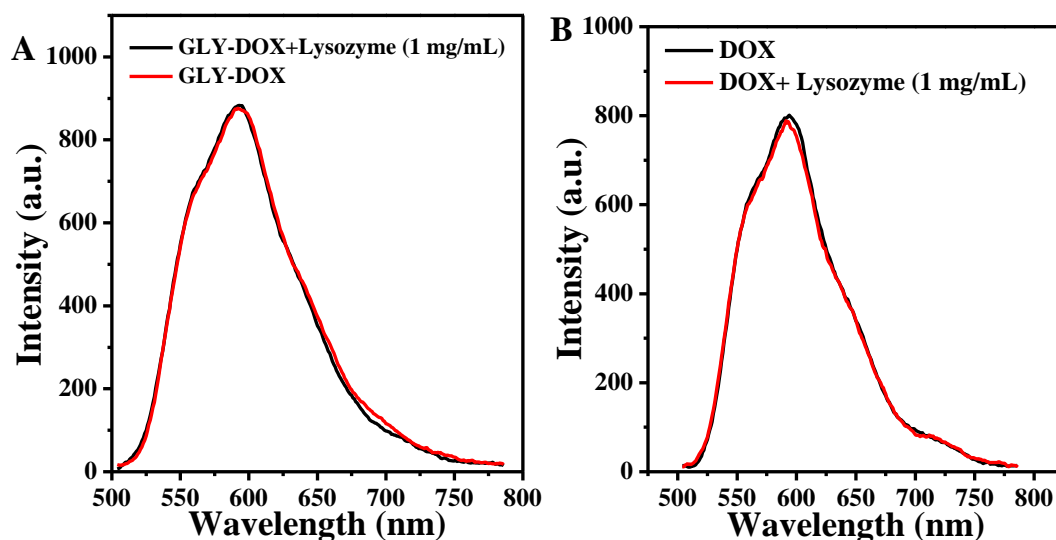


Fig. S6 The effect of lysozyme on the GLY-DOX and DOX by fluorescence spectra.

### Preparation of ND-PEG-DOX based on amide bond coupled DOX

ND-PEG-COOH (10 mg) was dispersed into deionized water (10 mL) under sonication for 30 min to form a suspension, and then added EDC (2.0 mg) and NHS (2.5 mg). Next, DOX (3.0 mg) dissolved sterilized double-distilled water was added dropwise, and a few drops of triethylamine was subsequently added to make the system pH about 8~9. After stirring for 24 hours at 37 °C under dark, ND-PEG-DOX was prepared successfully by centrifugation at 15000 rpm for 5 min, washed with deionized water and anhydrous methanol, respectively, until the supernatant was colorless, and then placed in the vacuum drying oven. The amount of DOX coupled in ND-PEG was measured (about 150  $\mu\text{g}/\text{mg}$ ) by using a UV-vis spectrophotometer at 480 nm according to the previous work.

### In vitro drug release of ND-PEG-DOX

The DOX release study was carried out in dialysis bags at 37 °C in acetate buffer solutions (pH 4.5, containing 1.0 mg/mL of lysozyme) with air oscillator (THZ-22,

Taicang City Experimental Equipment Factory). Firstly, 1 mL ND-PEG-DOX suspension with well dispersed in dialysis bags was placed in a centrifuge tube and quickly immersed in 9 mL of the corresponding acetate buffer solutions with a stirring of 150 rpm at 37 °C. At the scheduled time, 2 mL sample was withdrawn and the same amount of fresh release medium was replenished. The amount of released DOX was measured by above method to determine the cumulative release rate.

As displayed in Fig. S7, the release of DOX from ND-PEG-DOX was nearly 20% even after 50 h of incubation. The results strengthen our expectation that the amide bond-based conjugate will be stable at pH 4.5 in the presence of lysozymes (to mimic the endosomal conditions).

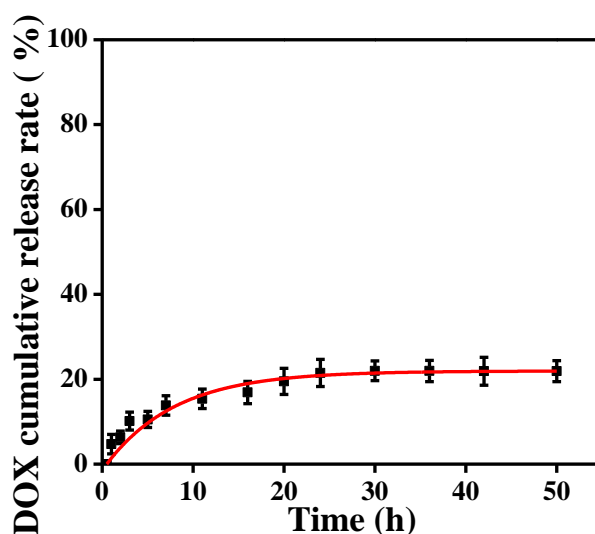


**Fig. S7** The cumulative release curve of ND-PEG-DOX in acetate buffer solutions (ABS) containing 1.0 mg/mL of lysozyme (pH 4.5).

### **Cell uptake of time-dependent by flow cytometer**

MCF-7 cells were seeded in 35 mm culture dishes at a density of  $1 \times 10^6$  per dish and allowed to attach overnight. Cells were then treated with NPGD at 37 °C for 1 h, 3 h,

5 h, 7 h and 16 h, respectively, after that cells were harvested by centrifugation (1000 rpm, 5 min) and the collected cells were washed thrice with cold PBS (pH 7.4). The samples were then analyzed by flow cytometer. A minimum of 10000 cells were analyzed. The fluorescence from the NPGD was excited at a wavelength of 488 nm and the emission was collected in the red light signal range. The fluorescence intensity was quantified by Cell Quest software.

To further examine the uptake ability of NPGD in cancer cells, MCF-7 cells were treated with the same concentrations of NPGD for different time and analyzed by flow cytometer. As shown in Fig. S8, the cellular uptakes of NPGD and free DOX were greatly strengthened with time increasing and reached a plateau at about 7 h for NPGD and 3 h for free DOX. Curve fitting by single exponent function showed that the rate constants ( $k$ ) of the endocytosis for NPGD was about  $0.316 \text{ h}^{-1}$ , namely, the value of uptake half-life was near 2.19 h, while the value of uptake half-life of free DOX was about 0.93 h, which indicated that the uptake rate of NPGD was approximately two times slower than free DOX. However, after 6 h, the uptake of the NPGD nanoparticles significantly improved (Fig. S8). These results are related to cellular uptake pathways. The uptake of DOX occurs through an energy-independent passive diffusion mechanism, while the NPGD nanoparticles can efficiently delivery the drug inside living cells via caveolae-dependent endocytosis pathway (Fig. 3E).

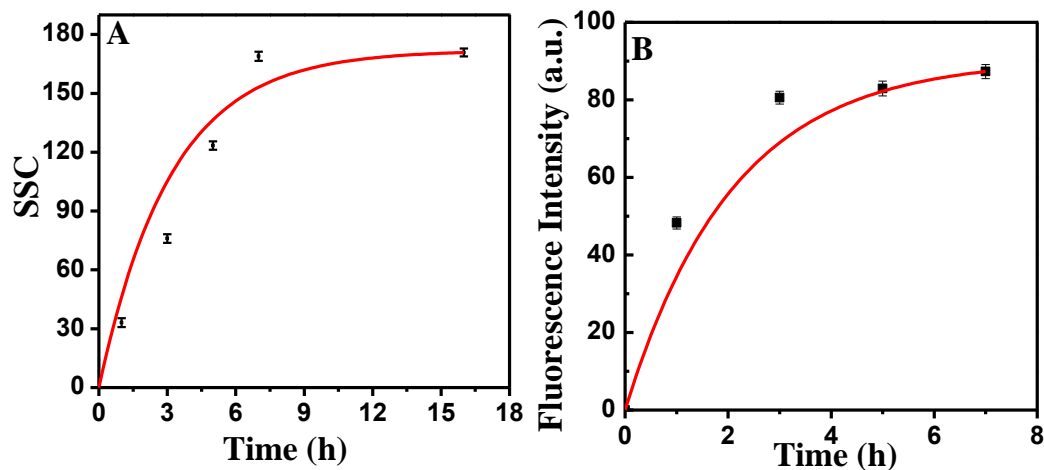


**Fig. S8** The kinetics of the cellular uptake of (A) NPGD and (B) free DOX.

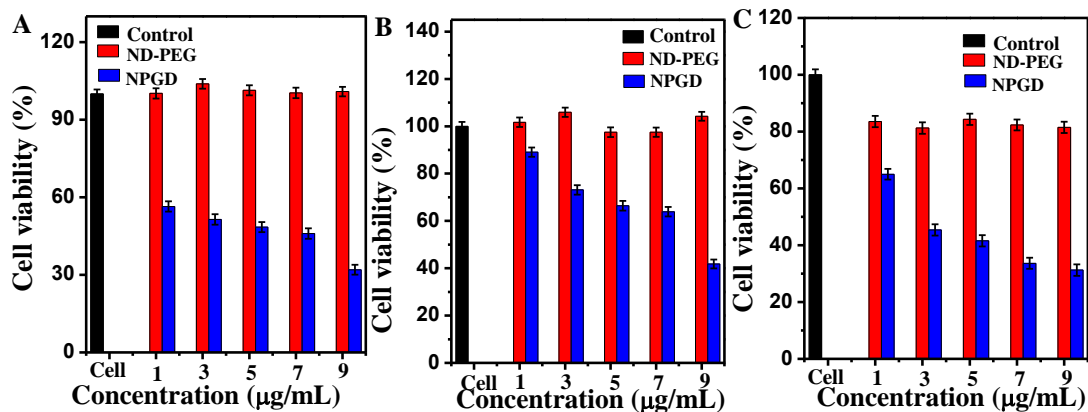


**Fig. S9** Effect of NPGD (The equivalent concentrations of GLY-DOX are 1, 3, 5, 7 and 9 µg/ml) and ND-PEG (The concentrations of ND-PEG are 7, 20, 34, 47 and 60 µg/ml) on HepG2, HeLa and MCF-7 cells viability for 72 h were measured by MTT assay. (A) HepG2 cells, (B) HeLa cells and (C) MCF-7 cells. Experiments were repeated three times and data are presented as the mean  $\pm$  SD (for each group,  $n = 6$ ).

### In vitro wound scratch

MCF-7 cells ( $2 \times 10^5$  cells per well) were seeded into 35 mm culture dishes and incubated overnight at 37 °C, allowing cells to adhere and spread on the substrate completely. Then scrape the cell monolayer in a straight line to create a “scratch” with a 10 µL pipet tip and remove the debris and smooth the edge of the scratch by washing the cells thrice with 1 ml of the PBS (pH 7.4), following the cells were



treated with NPGD at 37 °C. The dishes can be taken out of the incubator to be examined periodically and then returned to resume incubation. After the incubation, the cells were placed under a phase-contrast microscope to acquire images. Migration rate was expressed as percentage of scratch closure on an initial area basis, according to the following equation:

$$WC = \left(1 - \frac{SW_t}{SW_0}\right) \times 100\%, \text{MIR} = \left(1 - \frac{WC_{\text{treatment}}}{WC_{\text{control}}}\right) \times 100\%$$

where  $SW_0$  and  $SW_t$  stand for the scratch width of 0 h and given time, respectively,  $WC_{\text{treatment}}$  and  $WC_{\text{control}}$  stand for the wound closure rate of treatment and control groups.

To determine the effect of cell migration by NPGD, the scratch assays were performed in the presence of NPGD (5  $\mu\text{g/mL}$  of DOX equivalent). As shown in Fig. S10A, the scratch width is evidently narrowed while MCF-7 cells treated by ND-PEG even if time increases, which is similar to the control group. However the scratch width is nearly essentially unchanged while MCF-7 cells treated with NPGD and DOX, the migration inhibiting rate of NPGD and DOX were up to 90.1% and 82.32% as shown in Fig. S10B, respectively. Therefore, the NPGD can inhibit cell migration effectively.

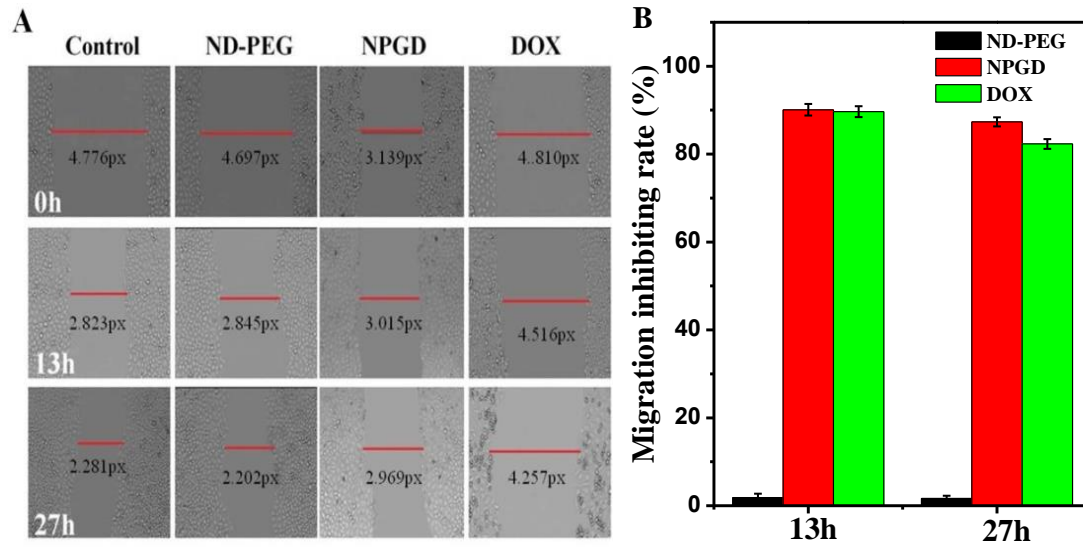


**Fig. S10** Effect of free DOX and NPGD on MCF-7 cells migration inhibition by in vitro wound scratch assay with time. (A) Representative images of MCF-7 cells treatment by NPGD and free DOX, and MCF-7 cells untreated as controls. (B) The plot was obtained by migration inhibiting rate vs. time, where data were adopted from (A).

### Cell apoptosis and cell cycle

MCF-7 cells ( $1 \times 10^5$  cells per well) were seeded in 35 mm culture dishes and allowed to attach overnight. Cells were then incubated at 37 °C for 48 h and 100 h with media containing NPGD at 5  $\mu$ g/mL of DOX equivalent, after that, cells were harvested by centrifugation (1000 rpm, 5 min). Collected cells were washed thrice with cold PBS (pH 7.4). For the apoptosis assay, the cells were rinsed twice with PBS and mixed with an equal volume of double staining solution AnnexinV-FITC and propidium iodide (PI) for 15 min at room temperature in the dark. Apoptosis was measured with a FACS Calibur flow cytometer.

MCF-7 cells ( $2 \times 10^6$  cells per well) were seeded in 35 mm culture dishes and allowed to attach overnight. Cells were then incubated at 37 °C for 30 h

with media containing NPGD at 5 µg/mL of DOX equivalent, after that, cells were harvested by centrifugation (1000 rpm, 5 min). Collected cells were washed thrice with cold PBS (pH 7.4) and fixed in 75% cold ethanol at 4 °C for overnight. For the cell cycle assay, the cells were rinsed twice with PBS and treated with propidium iodide (PI) solution containing RNase for 30 min at room temperature in the dark. Cell cycle was measured with a FACS Calibur flow cytometer. The DNA content of cell cycle phases which can be separated into G0/G1, S and G2/M was determined using Cell Quest Pro software.

Annexin V–FITC/PI double staining was used for determining whether NPGD has the same apoptotic effects as free DOX. The MCF-7 cells were treated with ND-PEG, NPGD and free DOX for 48 h and 100 h, respectively, and then subjected to simultaneous staining and analyzed by flow cytometry. As shown in Fig. S11A, ND-PEG (b, f) had hardly induced cell apoptosis similar to blank control (a, e), which verified its excellent biocompatibility and is also highly consistent with their in vitro wound scratch assay results (Fig. S10). On the contrary, the ratio of viable cells decreased and apoptotic cells increased when MCF-7 cells were treated with NPGD (c, g) and free DOX (d, h). From Fig. S11A (i), we can see that the NPGD (20.76%) was no match for free DOX (38.26%) when the incubation time was 48 h, but amazing, as the time up to 100 h, the NPGD had the same effect on apoptosis of MCF-7 cells (99.32%) as free DOX (98.99%). The results again confirmed that DOX could

efficiently release from NPGD and resulted in cell apoptosis, and NPGD system has a slow and sustain drug release capability.

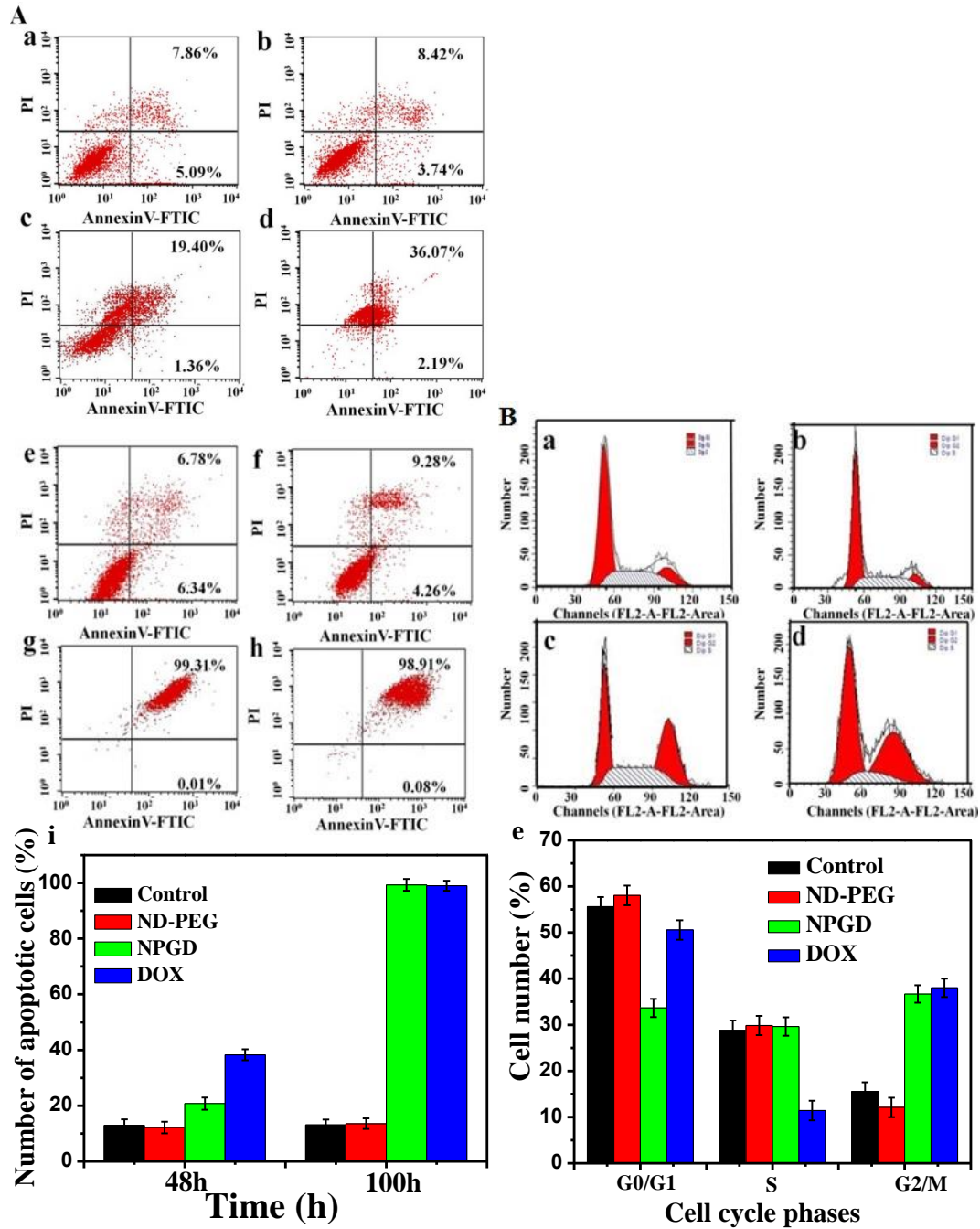


**Fig. S11** Flow cytometry analysis. (A) Apoptosis of MCF-7 cells induced by ND-PEG (b, f), NPGD (c, g) and DOX (d, h) for 48 h and 100 h, respectively, MCF-7 cells untreated as control (a, e), the number of apoptotic cells (i), where data were adopted from a-h. (B) Cell cycle of MCF-7 cells induced by ND-PEG (b), NPGD (c) and DOX (d), MCF-7 cells untreated as control (a), the cell cycle histogram (e), where data were adopted from a-d.

The cell cycle distributions of MCF-7 cells were also determined by flow cytometry. As shown in Fig. S11B, the cells treated with ND-PEG exhibited similar cell cycle with control cells, while NPGD (c) and free DOX (d) significantly changed the cell cycle, resulting in 21.96% and 5.06% reduction in the percentage of G0/G1 phase, 21.12% and 22.44% increase in the percentage of G2/M phase, respectively. From Fig. S11B (e), we can see that the cells treated with NPGD and free DOX all increased at the percentage of G2/M phase, which implied that NPGD and free DOX can change the cell cycle and mainly block in G2/M phase.